# Numerical and experimental exploration of phase control of chaos

Samuel Zambrano
*Nonlinear Dynamics and Chaos Group, Departamento de Matemáticas y Física Aplicadas y Ciencias de la Naturaleza, Universidad Rey Juan Carlos, Tulipán, s/n, 28933 Móstoles, Madrid, Spain*

Enrico Allaria
*Department of Physics, Università di Firenze, Firenze, Italy, and Istituto Nazionale di Ottica Applicata, Largo E. Fermi, 6 50125 Firenze, Italy*

Stefano Brugioni
*Istituto Nazionale di Ottica Applicata, Largo E. Fermi, 6 50125 Firenze, Italy*

Immaculada Leyva
*Nonlinear Dynamics and Chaos Group, Departamento de Matemáticas y Física Aplicadas y Ciencias de la Naturaleza, Universidad Rey Juan Carlos, Tulipán, s/n, 28933 Móstoles, Madrid, Spain*

Riccardo Meucci
*Istituto Nazionale di Ottica Applicata, Largo E. Fermi, 6 50125 Firenze, Italy*

Miguel A. F. Sanjuán[a)]
*Nonlinear Dynamics and Chaos Group, Departamento de Matemáticas y Física Aplicadas y Ciencias de la Naturaleza, Universidad Rey Juan Carlos, Tulipán, s/n, 28933 Móstoles, Madrid, Spain*

Fortunato T. Arecchi
*Department of Physics, Università di Firenze, Firenze, Italy, and Istituto Nazionale di Ottica Applicata, Largo E. Fermi, 6 50125 Firenze, Italy*

(Received 12 April 2005; accepted 2 December 2005; published online 13 January 2006)

A well-known method to suppress chaos in a periodically forced chaotic system is to add a harmonic perturbation. The phase control of chaos scheme uses the phase difference between a small added harmonic perturbation and the main driving to suppress chaos, leading the system to different periodic orbits. Using the Duffing oscillator as a paradigm, we present here an in-depth study of this technique. A thorough numerical exploration has been made focused in the important role played by the phase, from which new interesting patterns in parameter space have appeared. On the other hand, our novel experimental implementation of phase control in an electronic circuit confirms both the well-known features of this method and the new ones detected numerically. All this may help in future implementations of phase control of chaos, which is globally confirmed here to be robust and easy to implement experimentally. © *2006 American Institute of Physics*.
[DOI: 10.1063/1.2161437]

**Phase control of chaos is a chaos control method applied to periodically driven chaotic systems, where the key parameter is the phase difference between the main driving and an applied harmonic perturbation. Here we focus on a paradigmatic system of this type, the Duffing oscillator, to make a thorough study of this technique. Previous works on this method [Qu *et al.*, Phys. Rev. Lett. 74, 1736 (1995); Yang *et al.*, Phys. Rev. E 53, 4402 (1996)] show that a correct choice of the phase allows one to minimize the amplitude of the applied perturbation necessary to suppress chaos, and it can lead the system to a variety of periodic orbits. However, from our numerical exploration new interesting properties have arisen that should be taken into account in future implementations of this chaos control scheme. For example, we have observed that this method is strongly affected by the symmetries of the system. We have also noticed that a correct selection of the phase sometimes allows one to lead our system to a periodic orbit just for a very narrow interval of values of the perturbation amplitude, and that in some cases the eligible range of values of the phase that assure chaos suppression decreases as the perturbation amplitude grows. From our novel implementation of phase control in an analog circuit, we have obtained an experimental confirmation of both the known properties of this method and of the new ones, which strongly suggest that they are of quite a general nature. Our study contributes then to having a deeper insight into this technique, as well as to confirm its robustness and versatility.**

## I. INTRODUCTION

Chaotic behavior appears in many different contexts in a broad class of dynamical systems, either natural systems or man-made devices useful in science and technology. In general, chaos is an unwanted feature and as a consequence several control schemes have been devised in recent years, referred to in different ways as controlling chaos, suppressing chaos, or taming chaos. In any case, the goal of all these

[a)]Electronic mail: miguel.sanjuan@urjc.es

 

methods is to obtain a stable periodic orbit from a chaotic one by applying a small and accurately chosen perturbation to the system.[1]

The methods used to control chaos have been traditionally classified in two main groups: *feedback methods* and *nonfeedback methods*,[2] according to the way they interact with the system. Feedback methods of chaos control, OGY being the most representative,[3] attempt to stabilize the chaotic system in any of the unstable periodic orbits that lie in the chaotic attractor. However, in experimental implementations, the fast response that these methods require cannot usually be provided. In such cases, nonfeedback methods might be more useful.

Nonfeedback methods have been mainly used to suppress chaos in periodically driven dynamical systems. Among them a wide and important class is represented by those dissipative nonlinear oscillators whose general equation of motion may be written as

$$\ddot{x} + \delta\dot{x} + \frac{dV}{dx} = F\cos(\omega t), \tag{1}$$

where $\delta$ is the damping coefficient, $V(x)$ is the potential function responsible for the restoring force acting on the system, and $F\cos(\omega t)$ is an external periodic forcing. When $V(x)$ is the double-well potential, this equation represents the well-known Duffing oscillator. For this particular case and in absence of forcing and dissipation ($F=0$ and $\delta=0$), the phase space has at least one homoclinic point at (0, 0). Thus, under a suitable combination of external driving $F$ and dissipation $\delta$, the phase space presents transverse homoclinic points that may lead the system to a chaotic state.

The key idea of these nonfeedback methods is to apply a harmonic perturbation either to some of the parameters of the system or as an additional forcing, and its effectiveness is shown numerically and experimentally in several papers.[4–8] In one of these papers,[8] it was observed that the phase difference $\phi$ between the main driving and the perturbation had a certain influence on the global dynamics of the system, but in general the role of $\phi$ had been overlooked in the literature. However, Qu *et al.*[9,10] showed that $\phi$ influences drastically the global dynamics of the system. They proposed a control scheme that makes use of this property where $\phi$ acts as the control parameter: *phase control of chaos*.

We shall also point out that some theoretical efforts have been undertaken in order to understand the role of the harmonic perturbations, although essentially focused on how they contribute to frustrating transverse homoclinic orbits and then suppressing chaos[11–15] in the context of Melnikov theory.

Here we present an extensive numerical study and a novel experimental implementation of the phase control scheme by using the two-well Duffing oscillator as a paradigm. Our aim is to provide a more complete characterization of this type of chaos control, and to check out its validity in a real laboratory system: an electronic circuit. Two possible implementations of phase control of chaos are sketched in Fig. 1. For convenience we have decided here to explore the case in which a parametric perturbation is used [Fig. 1(b)].

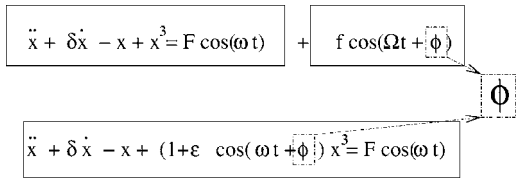


FIG. 1. Two possible implementations of phase control of chaos in a Duffing oscillator, (a) as an additive perturbation and (b) as a parametric perturbation. The phase difference $\phi$ between these perturbations and the main forcing is the key control parameter. We focus our attention on the case of a parametric perturbation throughout this paper.

Our numerical explorations confirm the main features of this method:[9,10] that an adequate choice of the phase leads the system from chaos to different periodic states, and how an accurate choice of $\phi$ can minimize the amplitude of the applied perturbation. However a thorough exploration of the parameter space allows us to find also new patterns on how phase control acts in this system, that were not previously observed. We underline the strong dependence of this control scheme on the symmetries of the system, and we can clearly visualize how the election of $\phi$ is strongly affected by the amplitude and the frequency of the harmonic perturbation.

Both the well-known features of phase control and the new ones are confirmed in the novel implementation of this scheme in a circuit that mimics the dynamics of the Duffing oscillator with a slight asymmetry. These results demonstrate that $\phi$ plays a role beyond the ideal symmetric case and strongly suggest that this type of chaos suppression can be useful for a wide variety of periodically driven systems.

The paper is organized as follows. In Sec. II we describe the model where the control method is applied. Numerical simulations showing the effect of the phase control in the system are presented in Sec. III. Section IV compares the numerical results with the experiment performed on the electronic circuit that mimics the Duffing oscillator. Finally, in Sec. V the main conclusions of our work are summarized.

## II. DESCRIPTION OF THE MODEL

As we mentioned in Sec. I, a paradigmatic system of the type described by Eq. (1) is the double-well Duffing oscillator, whose equation of motion reads

$$\ddot{x} + \delta\dot{x} - x + x^3 = F\cos(t). \tag{2}$$

Note that we take the value of the frequency of the external perturbation as $\omega=1$ throughout the paper. A well-known mechanical interpretation of this nonlinear oscillator is the motion of a unit mass particle in a double-well symmetric potential $V(x)=-x^2/2+x^4/4$ with dissipation and driven by an external periodic forcing. Depending on the values of $F$ and $\delta$, Eq. (2) yields a rich variety of dynamical solutions including stable equilibria, periodic oscillations, and chaotic solutions. We tailor the parameters $F$ and $\delta$ in such a way that its asymptotic state will be chaotic, and from then we study how to reach a periodic state under a suitable perturbation by using the phase control method.

To analyze the dynamics of Eq. (2) we numerically integrate it by using a fourth-order Runge Kutta algorithm with

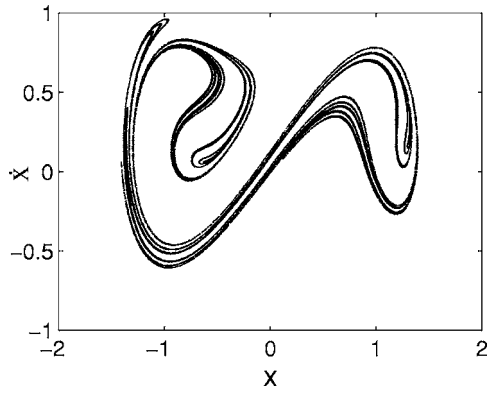


FIG. 2. A chaotic attractor of the nonlinear oscillator $\ddot{x}+0.15\dot{x}-x+x^3=0.258\cos(t)$. The value of the largest Lyapunov exponent is approximately 0.14.

500 integration steps per cycle, that is, with a time step $\Delta t=2\pi/500$. Once the trajectories are integrated, Lyapunov exponents can be calculated using standard techniques. We thus find that for the choice of parameters $F=0.258$ and $\delta=0.15$ the system is chaotic and its corresponding largest Lyapunov exponent is $\lambda\approx 0.14$. The Poincaré map of a typical trajectory is shown in Fig. 2. We keep these parameter values ($F=0.258$ and $\delta=0.15$) all throughout the numerical part of the paper.

As we have already affirmed, our aim here is to analyze the effects of the phase $\phi$ in the chaotic regime, when we add a harmonic perturbation. For this purpose we choose a harmonic parametric perturbation of the cubic term of the restoring force. Hence the complete equation of motion of our model is given by

$$\ddot{x}+\delta\dot{x}-x+(1+\epsilon\cos(rt+\phi))x^3=F\cos(t), \tag{3}$$

where $\epsilon\ll 1$ is the perturbation amplitude, $r$ is the ratio between the frequencies of the parametric modulation and the external forcing, and $\phi$ is the phase difference between the perturbation and the forcing. This modulation induces a slight harmonic variation of the width of the two wells and of the height of the potential barrier between the two minima of $V(x)$. Thus, $\phi$ can be interpreted also as the phase difference between this geometrical variation and the external forcing.

## III. NUMERICAL EXPLORATION OF PHASE CONTROL OF CHAOS

The equation that we use for the numerical simulations reads

$$\ddot{x}+0.15\dot{x}-x+(1+\epsilon\cos(rt+\phi))x^3=0.258\cos(t), \tag{4}$$

where $\epsilon$, $\phi$, and $r$ are free parameters. The main idea is that for $\epsilon=0$ the system is chaotic.

In order to better visualize the effect of the phase $\phi$ and how it has to be combined with the other parameters ($\epsilon$ and $r$) in the perturbation, we compute the largest Lyapunov exponent over every point in a $100\times 100$ grid in the region of parameters $0\leqslant\epsilon\leqslant 0.005$ $0\leqslant\phi\leqslant 2\pi$, fixing $r$ for each computation.

We have chosen such small $\epsilon$ values for our exploration to underline the effectiveness of phase control and to point out that in our system the chaos suppression mechanism considered cannot be the frustration of transverse homoclinic orbits (it is quite straightforward to show this by using the techniques exposed in Ref. 12). Our study is mainly focused on integer $r$ values as long as it has been shown that $r$ values of the form $r=q+\Delta q$ ($q$ integer), with $0<\Delta q\ll 1$, lead to an intermittency between chaotic and periodic motion referred to as *breather*.[9,10] We consider that by using these criteria we are covering most of the zones of interest of parameter space. We shall finally point out that special attention has been paid to avoid the transient states by waiting for a sufficiently long time to fix the corresponding stable regime, since we are searching for areas in the parameter plane where a transition between chaotic and regular motion takes place.

In Fig. 3 we plot the results for several integer $r$ values. The color assigned to each point in the $(\epsilon,\phi)$ parameter plane indicates whether for those parameter values Eq. (4) has a chaotic or a periodic solution. Instead of marking with two colors the points leading either to positive or negative Lyapunov exponents, we have chosen four different colors in order to better appreciate the structure of the chaos suppression regions. The black color denotes $\lambda<-0.025$, the grey color $-0.025\leqslant\lambda<0$, the silver color $0<\lambda<0.025$, and the white color $\lambda>0.025$.

Figure 3 shows that there exist wide regions of the $(\epsilon,\phi)$ plane where $\lambda$ is smaller than zero, and therefore chaos is suppressed. The most interesting characteristics of the phase control that were described in previous papers[9,10] are clearly present in this figure: the key role of the phase $\phi$ in selecting the final state of the system and how the use of a correct phase $\phi$ contributes to reduce the necessary $\epsilon$ value to suppress chaos. Consider for example the $r=2$ case [Fig. 3(b)], the maximal perturbation amplitude considered $\epsilon=0.005$ would not lead to a regular motion at $\phi=0$. Instead, at $\phi=3\pi/2$, a small value of the intensity as $\epsilon\approx 0.0025$ is enough to lead the system to a periodic state. However, there are other features that arise from the calculations shown in Fig. 3 that need to be emphasized.

First, we shall point out the key role of the symmetry of the system in the form of the control zones in the parameter plane. We can note that the control regions, far from having a trivial or irregular shape, present a symmetry that depends on the parity of the $r$ parameter: $\pi$ symmetry for odd r values [Figs. 3(a) and 3(c)] and the trivial $2\pi$ symmetry for even $r$ values [Figs. 3(b) and 3(d)].

In order to explain this difference related to parity in the control areas, we note that there exists a wide area of the phase space which verifies that both the point $(x_0,\dot{x}_0,t_0)$ and $(-x_0,-\dot{x}_0,t_0+\pi)$ belong to the same basin of attraction for a certain selection of the parameters $(\epsilon^*,\phi^*)$. In this region, the invariance of Eq. (2) under the transformation $x\mapsto -x$, $t\mapsto t+\pi$, $\phi\mapsto\phi+r\pi$ allows us to infer that if the system is controlled for a certain pair of values $(\epsilon^*,\phi^*)$, then chaos will also be controlled for $(\epsilon^*,\phi^*+r\pi \bmod (2\pi))$, as observed in Fig. 3.

Thus, the symmetries of the system can lead to two important advantages. First, they can be used to restrict the search of control areas to regions of the parameter plane of the form $0<\epsilon\leqslant\epsilon_0,\phi_0<\phi<\phi+r\pi$. Thus, in the $r=1$ and

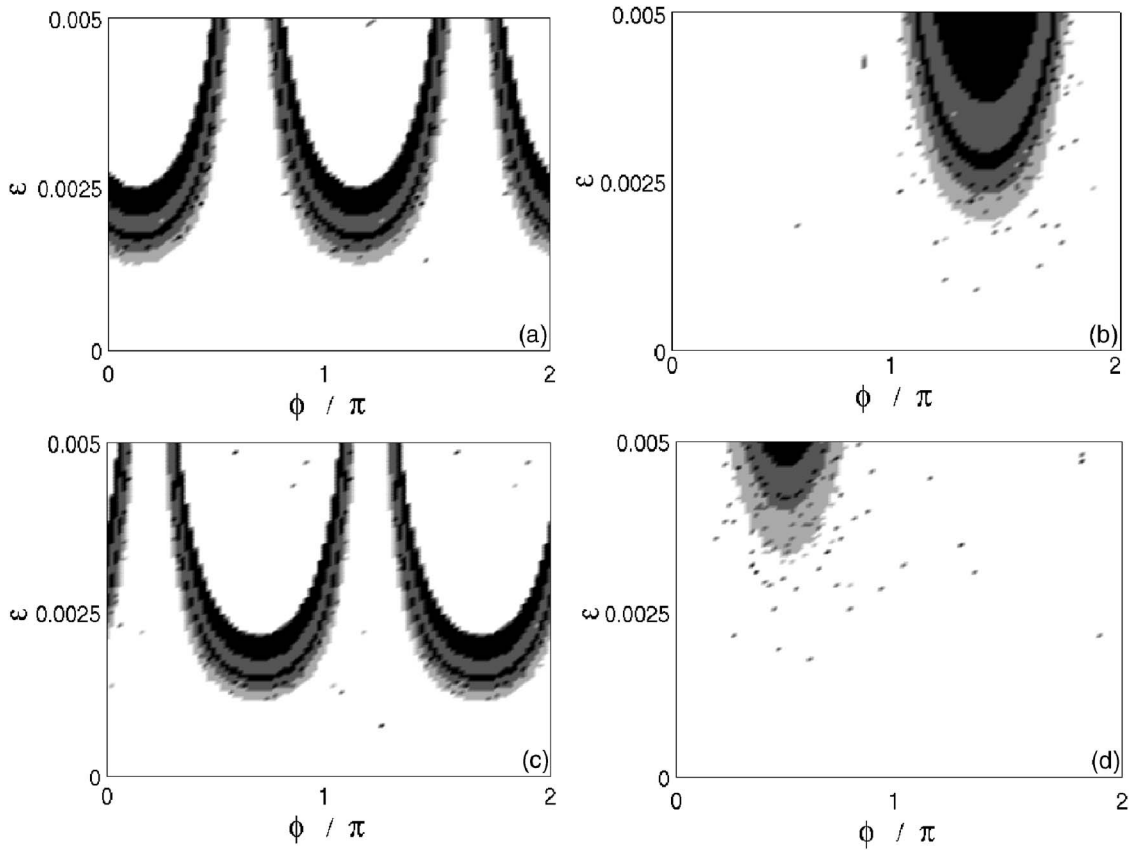


FIG. 3. Largest Lyapunov exponent λ computed at every point of a $100\times100$ grid of $(\epsilon,\phi)$ values in the region $0\leqslant\phi<2\pi$, $0\leqslant\epsilon\leqslant0.005$ for $\ddot{x}+0.15\dot{x}-x+(1+\epsilon\cos(rt+\phi))x^3=0.258\cos(t)$, fixing (a) $r=1$, (b) $r=2$, (c) $r=3$, (d) $r=4$. The black color denotes $\lambda<-0.025$, the grey color $-0.025\leqslant\lambda<0$, the silver color $0<\lambda<0.025$, and the white color $\lambda>0.025$. The control regions have a structure that follows the expected $\pi$ symmetry for $r$ odd and the trivial $2\pi$ symmetry for $r$ even.

$r=3$ cases we could have restricted our exploration to $\phi$ values in the interval $[0,\pi)$, as we can see in Figs. 3(a) and 3(c). On the other hand, the presence of these symmetries guarantee multiplicity of control regions in the $(\epsilon,\phi)$ for some $r$ values: it is evident that for $r=1$ and $r=3$ we have two control zones instead of one. However there are some cases where these two advantages are even more evident. For example, the $r=1/3$ case. In Fig. 4 we can see the calculation of λ as a function of $(\epsilon,\phi)$ for this $r$ value. Due to the global symmetry of the system, the control regions must present a $\pi/3$ symmetry on $\phi$. Thus, when the width of each of the six small control zones becomes sufficiently large ($\epsilon\approx0.0035$), the six control regions merge and chaos control is obtained nearly independently of the phase $\phi$. We shall point out that for other subharmonic frequencies explored, the required $\epsilon$ values were bigger.

From Fig. 3 other features showing that the phase $\phi$ must be combined with the other parameters in a nontrivial way can also be clearly visualized and have to be emphasized. We can observe there that a correct choice of $\phi$ does not assure chaos control for *all* $\epsilon$ values. That is, an appropriate choice of $(\epsilon,\phi)$ is fundamental. For example, in the odd $r$ cases [$r=1$ and $r=3$, Figs. 3(a) and 3(c)], it is clear that the choice of the $\phi$ value determines whether the final state of the system will be chaotic or periodic as in the even $r$ values. However, in these cases for a fixed $\phi$ value a continuous increasing of the perturbation amplitude $\epsilon$ can lead from a chaotic state to a periodic state and then back to chaos. Thus, contrary to what intuition may say, sometimes to increase $\epsilon$ from a periodic state, instead of rendering this state more stable, pushes the system toward chaos.

On the other hand, we can observe in Figs. 3(a) and 3(c), that the eligible $\phi$ range is reduced as $\epsilon$ increases. For ex-

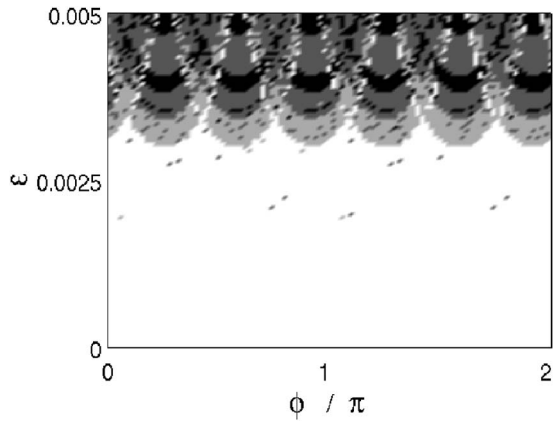


FIG. 4. Largest Lyapunov exponent λ computed at every point of a $100\times100$ grid of $(\epsilon,\phi)$ values in the region $0\leqslant\phi<2\pi$, $0\leqslant\epsilon\leqslant0.005$ for: $\ddot{x}+0.15\dot{x}-x+\left(1+\epsilon\cos\left(\frac{1}{3}t+\phi\right)\right)x^3=0.258\cos(t)$. The black color denotes $\lambda<-0.025$, the grey color $-0.025\leqslant\lambda<0$, the silver color $0<\lambda<0.025$, and the white color $\lambda>0.025$. Again, the control regions have a very interesting structure that follows the expected periodicity.

ample, for $r=1$ [Fig. 3(a)] two wide $\phi$ intervals of chaos suppression can be found for $\epsilon \approx 0.0025$, but if we increase $\epsilon$ to $\epsilon \approx 0.005$ we will only find four narrow ones. So another unintuitive feature arises from our exploration: by using bigger values of $\epsilon$, instead of finding wider $\phi$ intervals where chaos can be suppressed we may find narrower ones.

Up to this point, we have not said a word to characterize the stable state that is reached by our system when chaos is controlled. The numerical calculations shown in Fig. 3 do not allow us to identify the orbits to which the system is led for each choice of parameters $(\epsilon, \phi)$, but only to predict whether the system is chaotic or periodic. To distinguish the periodicity of the orbits, we compute bifurcation diagrams. We evaluate bifurcation diagrams fixing two particular values of $r$ and $\epsilon$ ($r=2$, $\epsilon=0.005$) and varying $\phi$. The results are shown in Fig. 5, where for the sake of clarity we plot just the local negative maxima of $x$ versus $\phi$. We note how the system can be driven to periodic orbits of different periods by suitably adjusting $\phi$, as was previously noticed in Refs. 9 and 10. Thus, varying $\phi$ is like "tuning" the system toward a desired periodic orbit. However we shall point out that, considering that the distance between the successive bifurcations decreases very fast and that the periodic windows are quite narrow, severe limitations may occur in experimental devices affected by noise. In this case only a few periodic orbits will be accessible.

## IV. EXPERIMENTAL EVIDENCE OF PHASE CONTROL OF CHAOS

Our goal here is to test the phase control method in a laboratory system, as well as to confirm the features that we have observed numerically. To this purpose, we build the electronic circuit sketched in Fig. 6. It consists of an electronic analog simulator implemented using commercial semiconductor devices. The variable $V_x$ is the output of $I_2$, while $V_y$ is the output of $I_1$. $V_d$ is the driving voltage amplitude applied by means of the generator $G_d$, while $V_c$ is the control voltage amplitude applied by $G_c$. The parameters $\omega_d$ and $\omega_c$ are the driving and control angular frequency, respectively. The integrators $I_1$ and $I_2$ have been implemented using Linear Technology LT1114CN four quadrant operational amplifiers, while the multipliers are Analog Devices MLT04. The acquisition of the experimental data has been performed by means of a LeCroy digital oscilloscope and by means of a real time acquisition board connected to a personal computer provided with LABVIEW software. $G_c$ is a digital-to-analog arbitrary wave form generator SONY TEKTRONIX AWG420. It can provide two wave forms of whatever shape. The generator can also control the phase difference $\phi$. Under a suitable normalization of the time scale the dynamics of this circuit is governed by Eq. (3), with a slight change in the values of the parameters $\delta=0.1471$, $F=0.262$, $\omega=1.257$. In this way, the variables $V_x, V_y$ can be associated to $x$, $\dot{x}$, respectively.

However, by observing the dynamics of the system with the aid of the oscilloscope we realize that the unperturbed ($\epsilon=0$) system does not follow exactly the expected chaotic dynamics described by Eq. (3). We observe that a typical trajectory spends more time in the region of negative values of the $x$ variable than in the region of the positive values, that is, it spends more time in the left well than in the right well, as shown in Fig. 7. This is equivalent to an asymmetrical double-well potential.

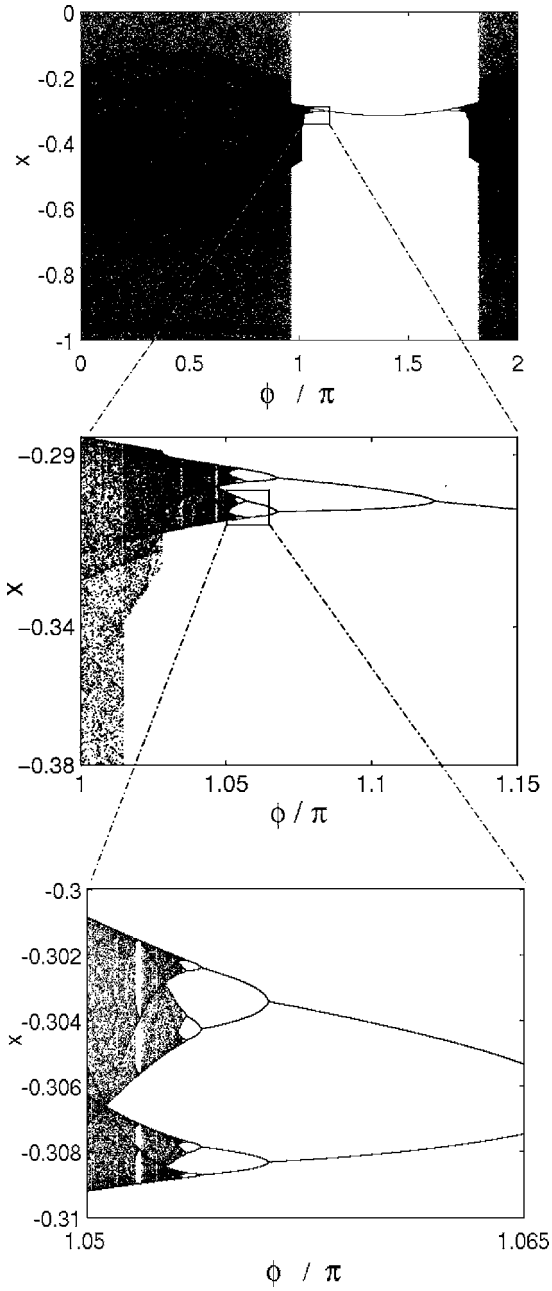


FIG. 5. Successive zooms of a bifurcation diagram showing the local maxima of the negative $x$ values vs $\phi$, for the equation $\ddot{x}+0.15\dot{x}-x+(1+0.005\cos(2t+\phi))x^3=0.258\cos(t)$. The dependence of the periodic orbit on the $\phi$ value can be noted. The higher the period of the orbit, the narrower the $\phi$ interval where it can be reached. Periodic windows are also present inside the chaotic sea.

An explanation of this phenomenon is given considering how multipliers work. Real multipliers differ from ideal ones because operations such as $x^3$ are done as $(x-\Delta_1)(x-\Delta_2)(x-\Delta_3)+C$, where $\Delta_i, C \ll 1$. Thus, instead of doing $x^3$ our circuit made the following operation: $x^3 \mapsto x^3+ax^2+bx+c$. We

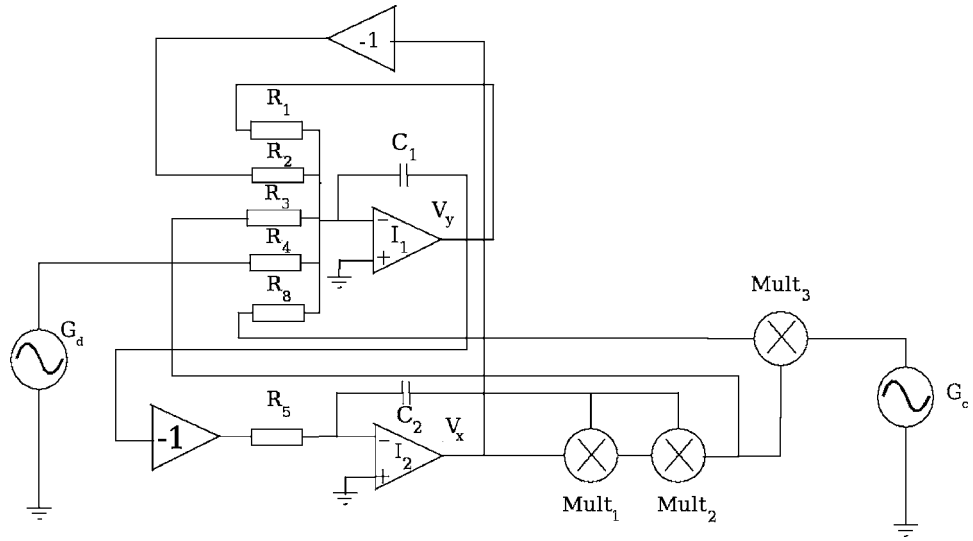


FIG. 6. Sketch of the electronic circuit. *I*: integrators; *R*: resistors; *C*: capacitors, Mult: multipliers; $G_d$: sinusoidal wave generator; $G_c$: arbitrary wave form generator. Under a suitable time normalization, the dynamics of the circuit is given by $\ddot{x}+0.1471\dot{x}-x+(1+\epsilon\cos(r1.257t+\phi))\,x^3=0.263\cos(1.257t)$, where $x\propto V_x$ and $\dot{x}\propto V_y$. The $\epsilon,\phi,r$ values can be fixed with the arbitrary wave form generator.

have made experimental measurements of the $x^3$ term provided for the multipliers, and furthermore we obtain the values: $a=-0.014$, $b=0.014$, $c=-0.12$ for the coefficients by using a polynomial fitting of the results.

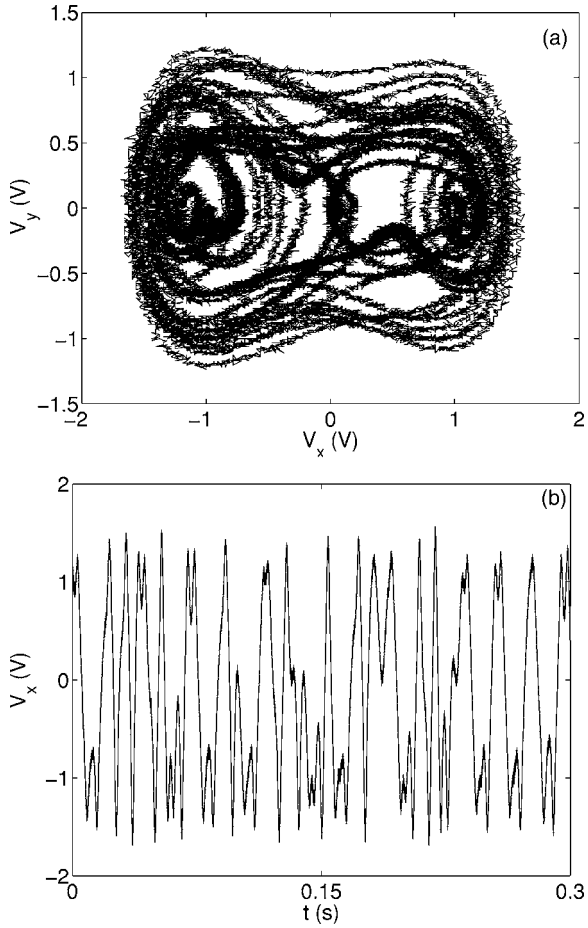


FIG. 7. (a) Experimental reconstruction of the chaotic attractor observed for the analog circuit. (b) Example of the experimental times series, where the asymmetry of the trajectory is observed.

Hence, the addition of these lower order terms besides $x^3$ in the restoring force makes the two-well potential $V(x)$ no longer symmetric, and consequently the left well becomes deeper than the right one. Thus, for the system it is more difficult to escape from the left well at $x<0$, where it spends more time. This is confirmed by Fig. 7(b), where an example of the experimental time series is shown.

Although in Sec. III we emphasized the advantages of global symmetries for control purposes, instead of considering this asymmetry as a problem we thought that this could be a good way to test the versatility and robustness of phase control of chaos. Following this strategy we repeat the numerical simulations considering the asymmetry in the potential. The new equation of the motion is

$$\ddot{x}+\delta\dot{x}-x+(1+\epsilon\cos(r\omega t+\phi))(x^3+ax^2+bx+C') = F\cos(\omega t). \tag{5}$$

In order to have a previous idea of the likely control areas, we test a wider region in the $(\epsilon,\phi)$ plane than in the ideal case. Thus, we explore the range of values $0\leqslant\epsilon\leqslant 0.03$ and $0\leqslant\phi\leqslant 2\pi$. We compute Lyapunov exponents for Eq. (5) on each point $(\epsilon,\phi)$ in a $100\times100$ grid in the considered region for different values of $r=1$, $r=2$, and $r=3$. The results are shown in Fig. 8.

Our numerical results confirm that the critical dependence on the phase $\phi$ to control chaos is preserved and that some of the previously observed features also apply to the asymmetric case. However, in the considered region, control islands of chaos suppression coexist with narrow control areas, and their structure is much more intricate and irregular than in the symmetric case. Due to the fact that the system does not present the invariance under the transformations described in the previous section for the symmetric case, the $r\pi$ symmetry of the control regions is no longer present as expected. Chaos is suppressed for a wide range of values of $\epsilon$, even for values below $\epsilon\leqslant 0.005$.

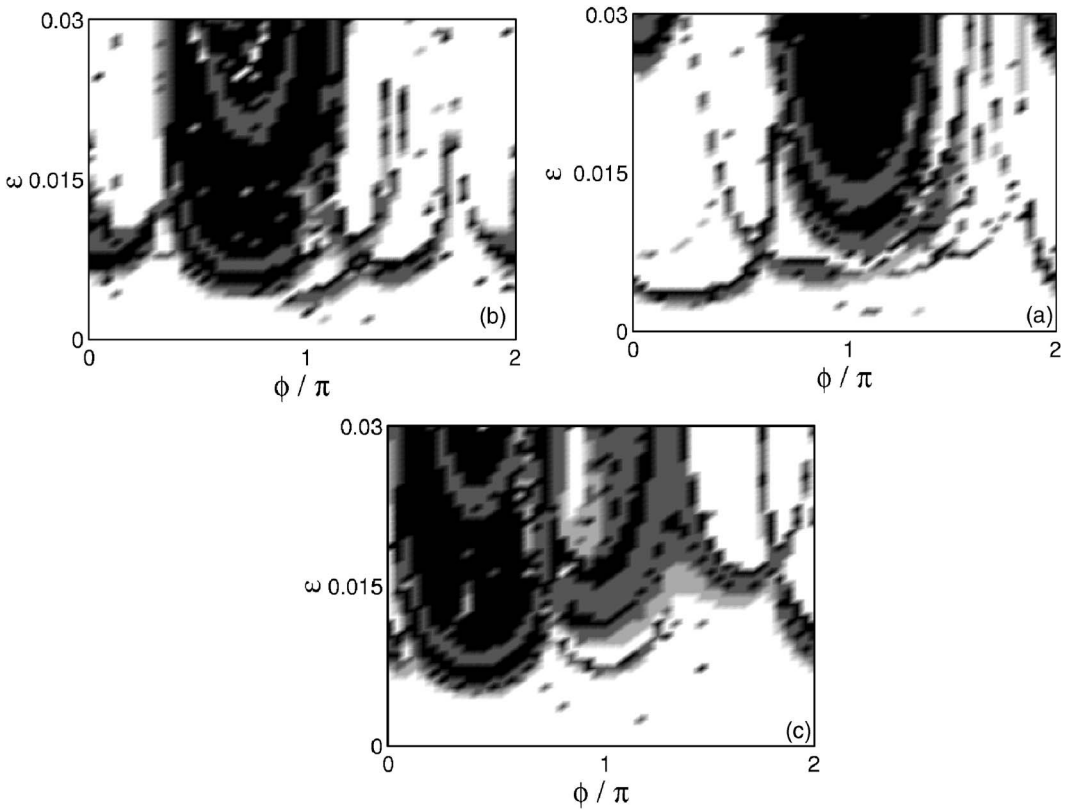


FIG. 8. Largest Lyapunov exponent λ computed at every point of a $100\times100$ grid of $(\epsilon,\phi)$ values in the region $0\leqslant\phi<2\pi$, $0\leqslant\epsilon\leqslant0.03$ considering the effective potential asymmetry: $\ddot{x}+0.147\dot{x}-x+(1+\epsilon\cos(1.257rt+\phi))(-0.12+0.014x-0.014x^2+x^3)=0.262\cos(t)$. The calculations have been made for (a) $r=1$, (b) $r=2$, (c) $r=3$. The black color denotes $\lambda<-0.025$, the grey $-0.025\leqslant\lambda<0$, the silver $0<\lambda<0.025$, and the white $\lambda>0.025$. The control regions lack the symmetry of the former case, but wide zones of chaos suppression do still appear.

Once we have a qualitative idea of the distortion induced by the potential asymmetry we can come back to the experiment. In our experiments we search for the control areas in the parameter space in an analogous way to what we did numerically. We detect and reconstruct these control areas by doing bifurcation diagrams fixing $r,\epsilon$ (for different $\epsilon$ values) and varying the phase value $\phi$. Such bifurcation diagrams are performed by searching for the maxima of the time series of the system obtained when the phase $\phi$ is slowly varied to the characteristic time scale of our system, that is, we make $\phi=\mu t$ with $\mu\ll1$.

The experimental control zones for $r=1$, $r=2$, and $r=3$ are observed in Figs. 9(a)–9(c). The main well-known characteristics of phase control of chaos are confirmed in our circuit: the crucial role of the phase $\phi$ on the final state and the smallness of $\epsilon$ needed to suppress chaos if $\phi$ is properly chosen. The new features analyzed previously are also present here. The lack of symmetry of the control regions due to the asymmetry of the potential is evident, so we can appreciate how the advantageous features observed from the symmetric case no longer apply here, as expected. On the other hand, the bifurcation in the control zone that appears in the $r=1$ case [Fig. 9(a)] confirms that the interesting patterns relating $\phi$ with the rest of the parameters of the harmonic perturbation do not only apply for the ideal symmetric case. We can also notice that the $\phi$ intervals where chaos is suppressed do roughly coincide with those predicted from numerical calculations. This is quite remarkable, as long as in our numerical simulations we did not consider any source of noise or instability.

## V. CONCLUSIONS

In this work we have performed a detailed analysis of a chaos control method, phase control of chaos, consisting of applying a small parametric harmonic perturbation to a periodically driven chaotic system and use the phase difference $\phi$ to vary the dynamical state of the system. We have focused our work in a paradigmatic system of this type: the Duffing oscillator.

We have performed numerical simulations confirming the most important properties of this method: that only a correct choice of $\phi$ can lead the system to a periodic orbit (once we fix the amplitude of the perturbation) and that, by adequately selecting the phase, the necessary amplitude to suppress chaos can be minimized. In practical applications, sometimes the range of accessible parameters within which the system can be perturbed is very narrow. Then, the phase represents an additional degree of freedom that becomes crucial to reach control.

With our numerical analysis we have also pointed out some features that were not observed in previous works on phase control of chaos. By using an extensive exploration of parameter space in search of zones of chaos suppression for different values of the perturbation amplitude $\epsilon$, resonance condition $r$, and phase $\phi$, we have detected some interesting

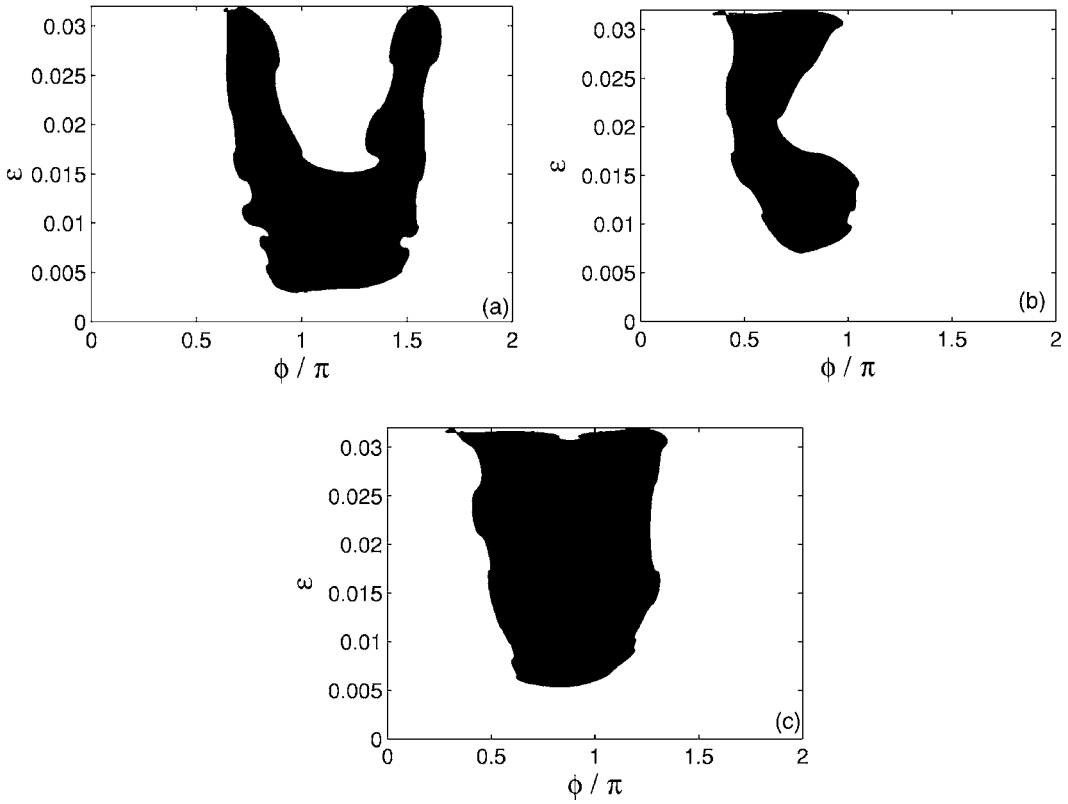


FIG. 9. Experimental control regions for the circuit of Fig. 5, reconstructed from experimental bifurcation diagrams, when (a) $r=1$, (b) $r=2$, (c) $r=3$. In spite of the experimental errors, there are still wide control zones that roughly coincide with those predicted by the numerical simulations.

patterns. The implementation of phase control in our system is a clear example of how the symmetries play a key role for this chaos control method, and of how they may be of great help in some cases. We have also observed how the phase $\phi$ sometimes has to be combined with the other parameters in a way that may be unintuitive and that is strongly affected by the values of the rest of the parameters of the perturbation applied. For example, we have seen that by increasing the perturbation amplitude $\epsilon$ sometimes we can lead the system from chaos to a periodic state and then back to chaos, and that sometimes the eligible range of $\phi$ values that stabilize the system in a periodic orbit becomes narrower as $\epsilon$ becomes bigger.

Most of the interesting patterns found numerically have been recovered in an experiment with an electronic circuit that mimics the dynamics of a Duffing oscillator with a slight potential asymmetry, even in the presence of noise. To our knowledge, no other verification of the validity of phase control of chaos in a real laboratory system had been performed before. This fact suggests that phase control of chaos is robust even in the presence of distortions of the potential symmetry and that all the properties observed in this work are of a quite general nature, so they must be taken into account when applying this control method to the most diverse dynamical systems.

The above-summarized characteristics and the observed robustness of this scheme in its implementation in the electronic circuit, together with the advantages derived from the nonfeedback nature of this method, make us think that phase control of chaos can be useful in many experimental situations where periodically driven chaotic systems appear, such as lasers or superconductor junctions.

## ACKNOWLEDGMENTS

This work has been supported by the Spanish Ministry of Science and Technology under Project No. BFM2003-03081 and by the Universidad Rey Juan Carlos under Project No. PPR-2004-28. E.A. was supported by FIRB Contract No. RBAU01B49F_002. Partial support from Azione Integrata Italia Spagna IT1348 and Acción Integrada Hispano-italiana HI03-207 is also acknowledged.

[1] T. Shinbrot, C. Grebogi, E. Ott, and J. A. Yorke, "Using small perturbations to control chaos," Nature (London) **363**, 411 (1993).
[2] S. Boccaletti, C. Grebogi, Y. C. Lai, H. Mancini, and D. Maza, "Control of chaos: Theory and applications," Phys. Rep. **329**, 103 (2000).
[3] E. Ott, C. Grebogi, and J. Yorke, "Controlling chaos," Phys. Rev. Lett. **64**, 1196 (1990).
[4] R. Lima and M. Pettini, "Suppression of chaos by resonant parametric perturbation," Phys. Rev. A **41**, 726 (1990).
[5] G. Gicogna and L. Fronzoni, "Effects of parametric perturbations on the onset of chaos in the Josephson-Junction model: Theory and analog experiments," Phys. Rev. A **42**, 1901 (1990).
[6] Y. Braiman and I. Goldhirsch, "Taming chaotic dynamics with weak periodic perturbations," Phys. Rev. Lett. **66**, 2545 (1991).
[7] L. Fronzoni, M. Giocondo, and M. Pettini, "Experimental evidence of suppression of chaos by resonant parametric perturbations," Phys. Rev. A **43**, 6483 (1991).
[8] R. Meucci, W. Gadomski, M. Ciofini, and F. T. Arecchi, "Experimental control of chaos by means of weak parametric perturbations," Phys. Rev. E **49**, R2528 (1994).

[9]Z. Qu, G. Hu, G. Yang, and G. Qin, "Phase effect in taming nonautonomous chaos by weak harmonic perturbations," Phys. Rev. Lett. **74**, 1736 (1995).
[10]J. Yang, Z. Qu, and G. Hu, "Duffing equation with two periodic forcings: The phase effect," Phys. Rev. E **53**, 4402 (1996).
[11]R. Chacón, "Suppression of chaos by selective parametric perturbations," Phys. Rev. E **51**, 761 (1995).
[12]R. Chacón, "Maintenance of chaos by weak harmonic perturbations: A unified view," Phys. Rev. Lett. **86**, 1737 (2001).
[13]R. Chacón, "Role of ultrasubharmonic resonances in taming chaos by weak harmonic perturbations," Europhys. Lett. **54**, 148 (2001).
[14]H. Cao, X. Chi, and G. Chen, "Suppressing or inducing chaos by weak resonant excitations in an externally-forced Froude pendulum," Int. J. Bifurcation Chaos Appl. Sci. Eng. **14**, 1115 (2004).
[15]A. Y. T. Leung and L. Zengrong, "Suppressing chaos for some nonlinear oscillators," Int. J. Bifurcation Chaos Appl. Sci. Eng. **14**, 1455 (2004).